Coordinate-Targeted and Coordinate-Stochastic Super-Resolution Microscopy with the Reversibly Switchable Fluorescent Protein Dreiklang

Nickels A. Jensen,[a] Johann G. Danzl,[a] Katrin I. Willig,[a] Flavie Lavoie-Cardinal,[a] Tanja Brakemann,[a] Stefan W. Hell,*[a] and Stefan Jakobs*[a, b]

1. Introduction

The resolution of far-field optical microscopy has long been limited by diffraction, which prevents light from being focused more sharply than to a spot of diameter ~λ/(2NA) with λ being the wavelength of light and NA the numerical aperture of the lens. Because diffraction is intrinsic to all wave propagation, the diffraction barrier was regarded as practically insurmountable. Within the last two decades, concepts for resolving fluorescent samples without diffraction limit have emerged, enabling fluorescence microscopy (nanoscopy) with resolution at the nanoscale.[1] These concepts overcome the diffraction limit by causing the fluorophores of neighboring features to briefly assume two different states, making them distinguishable; usually the two states are a fluorescent (on-) and a non-fluorescent (off-) state.[2]

A number of state transitions have been identified that can be exploited to distinguish identical fluorophores that are spatially closer than the diffraction limit. However, depending on how the transition is implemented, current fluorescence nanoscopy or super-resolution methods may be assigned to one of two classes, namely, those that are based on a light-induced coordinate-targeted state transfer and those that are based on a spatially stochastic single-molecule based switching and read-out.[1a,2] Prominent members of the former family of techniques are RESOLFT [reversible switchable optical linear (fluorescence) transitions][3] and STED (stimulated emission depletion) microscopy.[4] In RESOLFT and STED microscopy, a light pattern is used that transfers fluorophores briefly to one of these states (usually to the non-fluorescent state) at well-defined coordinates in space. In STED microscopy this is accomplished by stimulated emission of excited fluorophores to the ground state, whereas the generalized RESOLFT concept includes transient transfers of the fluorophore to metastable dark states. In RESOLFT and STED microscopy, the spatial coordinate range in which molecules are able to assume one of these states (usually the fluorescent one) is $d \approx \lambda/NA\sqrt{1 + I_{max}/I_S}$ defining the resolution. I_s is a characteristic of the fluorophore and I_{max} denotes the intensity of the peak enclosing the zero.[2] For $I_{max}/I_s \gg 1$, the resolution d fundamentally exceeds the diffraction limit. Hence, RESOLFT and STED microscopy differ only in the type of state transition modulating the fluorescence signaling. Whereas STED microscopy creates the state difference with relatively short-lived states, RESOLFT microscopy typically uses long-lived states for feature separation. Thus the light intensities used for switching in RESOLFT microscopy are typically by about 10^5 to 10^6 fold lower than in STED microscopy.

In the spatially stochastic super-resolution approaches, individual fluorophores are stochastically switched to the on-state and localized with subdiffraction precision using the many fluorescence photons emitted in the on-state. The localization

[a] *Dr. N. A. Jensen, Dr. J. G. Danzl, Dr. K. I. Willig, Dr. F. Lavoie-Cardinal, Dr. T. Brakemann, Prof. Dr. S. W. Hell, Prof. Dr. S. Jakobs*
Department of NanoBiophotonics
Max Planck Institute for Biophysical Chemistry
37070 Göttingen (Germany)
E-mail: shell@gwdg.de
sjakobs@gwdg.de

[b] *Prof. Dr. S. Jakobs*
Department of Neurology
University Medical Center of Göttingen
37073 Göttingen (Germany)

precision of single molecules scales approximately with the inverse square root of the number of photons detected from the single emitter. Images are assembled by registering the individual fluorophores with high precision at random locations. This family of methods typically requires the recording of up to several 10000 camera frames to collect and establish the position of a statistically representative number of molecules. The first implementations of this family of approaches were termed stochastic optical reconstruction microscopy (STORM),[5] photoactivated localization microscopy (PALM),[6] and fluorescence photoactivation localization microscopy (FPALM).[7] Switching mechanisms based on different state transitions have also been exploited since then, further expanding the repertoire of stochastic fluorescence nanoscopy. This includes ground-state depletion followed by individual molecule return (GSDIM; also called dSTORM) microscopy that transfers fluorophores from the bright singlet system to a long-lived dark state.[8] Altogether, both super-resolution classes require fluorophores to be transferred between different states, and fluorescent proteins have been widely used for this purpose.

An emerging class of high-potential fluorophores are the reversibly switchable fluorescent proteins (RSFPs).[9] These proteins are structurally similar to the green fluorescent protein (GFP), but can be switched reversibly by irradiation with different wavelengths between a non-fluorescent and a fluorescent state. This property has been used to overcome the diffraction barrier in RESOLFT nanoscopy in living cells by applying relatively low light intensities.[10] In conventional RSFPs such as Dronpa-M159T[11] or rsEGFP,[10b] fluorescence readout concomitantly induces switching. This entanglement is ultimately rooted in the switching mechanism, an optically induced reversible cis-trans isomerization of the chromophore that is often accompanied by a change in its protonation state.[9,12] Because of the entanglement of switching and fluorescence generation, conventional RSFPs are presumably less suited for methods relying on stochastic single molecule switching.

In the recently introduced RSFP Dreiklang, fluorescence readout and switching are disentangled.[10a] This is due to an entirely different molecular switching mechanism, namely a reversible light-induced water addition/elimination reaction occurring at the chromophore. Dreiklang is switched off with blue light (~405 nm), switched on with UV light (~350 nm) and the fluorescence is excited with ~515 nm. Using this light driven switching mechanism, Dreiklang has previously been exploited for both coordinate-targeted RESOLFT as well as for coordinate-stochastic super-resolution microscopy (DSSM: decoupled stochastic switching microscopy).[10a]

In this study we demonstrate that Dreiklang can in addition also be used for STED and GSDIM microscopy, which are coordinate-targeted and stochastic, respectively, and rely on different state transfers.

2. Results

2.1. Exploiting the Unique Switching Mechanism of Dreiklang for RESOLFT and DSSM Microscopy

To evaluate the usability of Dreiklang as a probe for super-resolution microscopy, we expressed a fusion protein consisting of Vimentin and Dreiklang in HeLa cells, a human cell line derived from a cervical cancer. Vimentin is a member of the intermediate filament protein family and Vimentin–Dreiklang forms an extended meshwork of fibers of variable widths in the HeLa cells. The meshwork can be very dense, making it challenging to resolve the finest fibers with confocal or widefield microscopy (Figure 1).

Relying on the reversible light-induced water addition/elimination reaction occurring at the chromophore to switch between the fluorescent and the non-fluorescent state, Dreiklang has been used in its initial demonstration for RESOLFT nanoscopy, but also for coordinate-stochastic super-resolution methods.[10a] To demonstrate that Vimentin–Dreiklang expressing cells are also better resolved when imaged with these two methods, we first imaged them by RESOLFT microscopy. To this end, a home-built RESOLFT microscope was used that provided a regularly focused focal light spot for switching Dreiklang into the on-state ($\lambda = 355$ nm; 1 ms; 0.3 kW cm^{-2}). A doughnut-shaped focal spot of blue light ($\lambda = 405$ nm; 17 ms, 10 kW/cm^2) with a central intensity minimum was used for switching Dreiklang off at the focal spot periphery. Finally, the fluorescence was probed by 491 nm excitation (2 ms, 0.8 kW cm^{-2}).

Images were generated by scanning over the sample using this irradiation scheme at every 30 nm sized pixel. Thin filaments were better resolved in the RESOLFT images than in the corresponding confocal counterparts (Figure 1a). Measuring several adjacent intensity profiles across thin filaments and fitting them with a Lorentzian function resulted in full width at half maximum (FWHM) of ~55 nm in case of thin filaments (Figure 1a). As the determined FWHM is co-determined by the actual thickness of the filaments, we conclude that the focal plane resolution was better than 50 nm in this living cell RESOLFT recording.

To use the Dreiklang-specific switching mechanism for stochastic super-resolution microscopy as well, we modified a commercial GSDIM microscope (Leica SR GSD) so that the sample could be irradiated with UV light of 365–375 nm provided by a 100W Hg lamp (in addition to the already available light of 405 and 488 nm provided by lasers). The availability of blue and UV light allows us to directly control the number of on-state molecules in the sample, providing an additional level of flexibility to adapt the imaging conditions to the fluorophore distribution in the sample. Because this immediate control requires a reversible light-driven switching mechanism whose switching is decoupled from the fluorescence excitation (as provided by Dreiklang), we refer to this specific super-resolution variant as decoupled stochastic switching microscopy (DSSM). For DSSM, the cells were initially irradiated for 1 s at 405 nm (0.2 kW cm^{-2}) to switch the majority of Dreiklang pro-

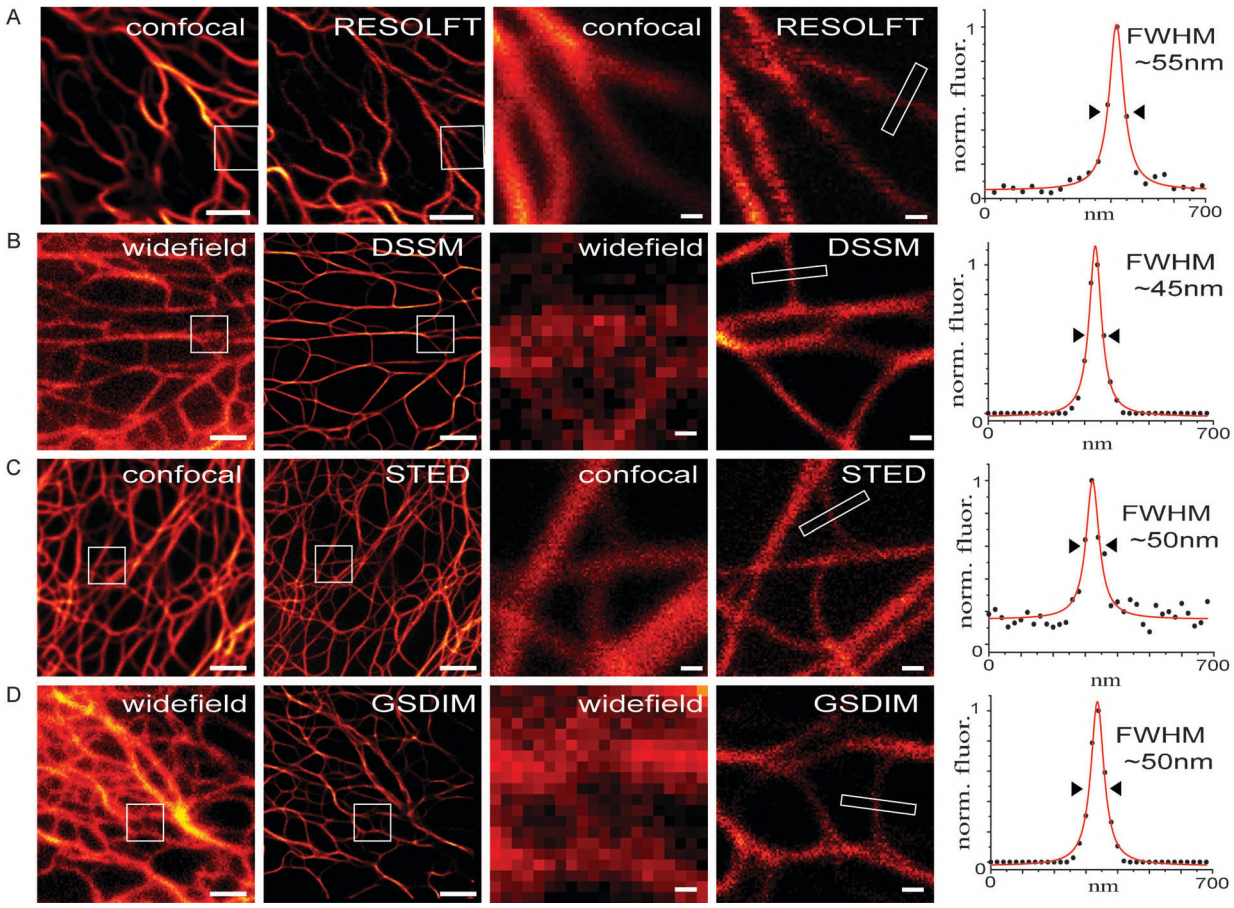

Figure 1. Live cell imaging of HeLa cells expressing Vimentin–Dreiklang using different super-resolution microscopy methods: A) RESOLFT (coordinate-targeted), B) DSSM (coordinate-stochastic), C) STED (coordinate-targeted), D) GSDIM (coordinate-stochastic). In all rows: Left: conventional (confocal or widefield) overview and the corresponding super-resolution image. Middle: magnifications of the areas indicated in the overview images. Right: four or five neighboring intensity profiles taken across a thin filament at the indicated sites (in the magnifications) were averaged and fitted with a Lorentzian function. The FWHM was determined from this fit. The final nanoscopy images were recorded (RESOLFT, STED) or calculated (DSSM, GSDIM) with a pixel size of 20 nm (STED, DSSM, GSDIM) or 30 nm (RESOLFT). Scale bars: 2 μm (overview images) and 200 nm (magnifications).

teins off. Subsequently, we recorded 20000 image frames (10 ms each) with irradiation at 488 nm (3 kW cm^{-2}). Based on the number of detected photons (~400 per individual burst), the obtained theoretical localization precision was <20 nm,[13] resulting in final images that were clearly superior to the conventional counterparts (Figure 1 b). The FWHM of thin Vimentin–filaments was ~45 nm, which is comparable to the value measured by RESOLFT nanoscopy on a different cell. The measured FWHM is substantially larger than the localization precision, suggesting that also in this case the structure limits the resolution obtained. We conclude that the reversible photoswitching with blue and UV light exploiting the unique photochemical switching mechanism of Dreiklang can be used to overcome the diffraction barrier in living cells both by coordinate-targeted imaging as well as by coordinate-stochastic super-resolution microscopy.

2.2. STED Nanoscopy with Dreiklang

Dreiklang has been derived from the fluorescent protein Citrine,[14] which reportedly is among the most suited fluorescent proteins for STED microscopy.[15] We reasoned that Dreiklang may also be well suited for STED microscopy. To test this, living cells expressing Vimentin–Dreiklang were imaged with a home-built STED microscope.[15] Dreiklang was excited at 488 nm and STED was applied at 595 nm. We found Dreiklang usable for STED microscopy and found it at least as photostable as Citrine under these imaging conditions. Generally, 4–6 STED images could be recorded of a living cell expressing Vimentin–Dreiklang. Thin filaments imaged in the STED mode had a diameter of ~50 nm (Figure 1 c). Hence, also STED microscopy can be performed with Dreiklang as a fluorescence probe, relying on an entirely different switching mechanism as in RESOLFT or DSSM.

2.3. GSDIM with Dreiklang

Next, we investigated whether Dreiklang could also be utilized for GSDIM, which operates in a spatially stochastic mode.[8a] In this approach, laser light (here $\lambda = 488$ nm), is used to transfer the fluorophores from the singlet ground state (S_0) into a long-lived dark state, via the excited state S_1. From this dark

state they return stochastically in time and space back to the ground state and their positions are determined after recording the fluorescence signal on a camera. This coordinate-stochastic approach does not require any additional laser line for switching and is performed in living cells. Cells were imaged in $DMEM^{GFP}$ growth medium to reduce photobleaching.[16] As previously observed with RESOLFT, DSSM and STED, we also measured ~50 nm FWHM on thin filaments that were recorded with GSDIM (Figure 1 d). We therefore conclude that Dreiklang may also be used for GSDIM microscopy relying on yet another optically driven on–off switching mechanism.

2.4. Comparison of Coordinate-Stochastic GSDIM and DSSM Utilizing Dreiklang

Comparing cells expressing Vimentin–Citrine or Vimentin–Dreiklang, we found that the labeling efficiency and the overall expression levels of Dreiklang and Citrine were similar. Also, using the same irradiation scheme and the same optical intensities for GSDIM, we found that the number of emitted photons per single fluorescence burst from Dreiklang or Citrine were comparable (~400 photons), enabling a theoretical localization precision[13] of <20 nm for both proteins (Figure 2). However, Dreiklang generally enabled the recording of more image frames than Citrine, indicating stronger resistance to photobleaching (Figure 2 a, b).

As a coordinate-stochastic method, DSSM is conceptually similar to GSDIM but relies on a different switching mechanism as detailed above. Nonetheless, presumably, also in DSSM, a number of on-state Dreiklang molecules are transferred by the 488 nm probing light into a long-lived dark state, followed by spontaneous relaxation back into the fluorescent state as in GSDIM. The degree of GSDIM-like switching will depend on the probing light intensity and the wavelength used. Imaging by DSSM also led to an average number of ~400 emitted photons per burst (Figure 2 d). A side-by-side comparison of DSSM and GSDIM using the same samples expressing Vimentin–Dreiklang generally showed a similar number of blinking events in the first ~10000 image frames recorded. However, in later image frames, comparatively more blinking events were recorded when the cells were imaged in the DSSM mode, even when we did not activate Dreiklang additionally at 370 nm (Figure 2 b–d). We attribute the larger number of recorded blinking events to reduced photobleaching in case of the photochemical switching to the off-state ($\lambda = 405$ nm; 1 s; 0.2 kW cm^{-2}) in DSSM as compared to switching into a dark state from the S_0 via the S_1, as in GSDIM ($\lambda = 488$ nm; 10 s; 3 kW cm^{-2}), requiring much higher light intensities albeit with light of longer wavelength.

Altogether, we regard Dreiklang superior for live cell coordinate-stochastic imaging when compared to Citrine, which has been reported to be among the best suited fluorescent proteins for GSDIM.[15]

3. Discussion

Dreiklang may be reversibly transferred by any one of the three distinct light-driven photochemical or photophysical pathways into different dark states, namely, by a reversible optically induced water addition/elimination reaction occurring at the chromophore, by stimulated emission, or by transferring the chromophore with strong excitation light from the S_0 ground state into a long-lived dark state. We demonstrated that all three switching mechanisms can be used to overcome the diffraction barrier either in a coordinate-targeted and/or a coordinate-stochastic approach (Figure 3). Presumably, this collection of Dreiklang applications could be further extended to methods that also rely on stochastic blinking of fluorophores such as super-resolution optical fluctuation imaging (SOFI),[17] and others.[18]

Dreiklang is a versatile RSFP that proved to be usable for different super-resolution methods providing comparable sub-diffraction resolution in living cells. However, because Dreiklang has not been optimized specifically, it may not necessarily be used to directly compare the different imaging perfomances of the various super-resolution methods. Based on previous mutagenesis efforts aimed at improving other RSFPs,[10b] it can be anticipated that Dreiklang may be further improved at least with respect to switching fatigue and speed, which would be especially beneficial for RESOLFT microscopy.

In STED imaging and GSDIM, Dreiklang bleached less compared to its progenitor Citrine. This effect might be explained by the additional switching pathway offered by Dreiklang that may open up a further pathway to avoid irreversible destruction. In DSSM, the reversible photochemical switching requires orders-of-magnitude-lower light intensities than those needed in GSDIM imaging, whereas at the same time it offers additional degrees of freedom to adjust the imaging conditions, enabling the recording of more blinking events and thus higher quality images.

Experimental Section

Sample Preparation

The mammalian expression plasmids pVimentin–Citrine and pVimentin–Dreiklang were constructed by a gateway vector conversion system using pDONR223-Vim, as described previously.[10a] HeLa cells were cultured at 37 °C with 5% CO_2 in DMEM (Invitrogen, Carlsbad, USA) containing 10% FCS (PAA Laboratories, Cölbe, Germany), 1 mM pyruvate (sigma, St-Louis, USA), 100 U mL^{-1} streptomycin and 100 μg mL^{-1} penicillin (Biochrom Berlin, Germany). Cells were seeded on coverslips in six well plates and transiently transfected with the plasmids using Turbofect (Thermo Scientific, Waltham, USA) the following day according to the manufacturer's instructions. 24 to 48 h after transfection, the cells were transferred in $DMEM^{gfp}$ (Evrogen Moscow, Russia), mounted on concavity slides and sealed with twinsil (Picodent, Wipperfürth, Germany).

GSDIM and DSSM

GSDIM and DSSM studies were performed with a custom modified Leica SR GSD microscope (Leica Microsystems, Wetzlar, Germany)

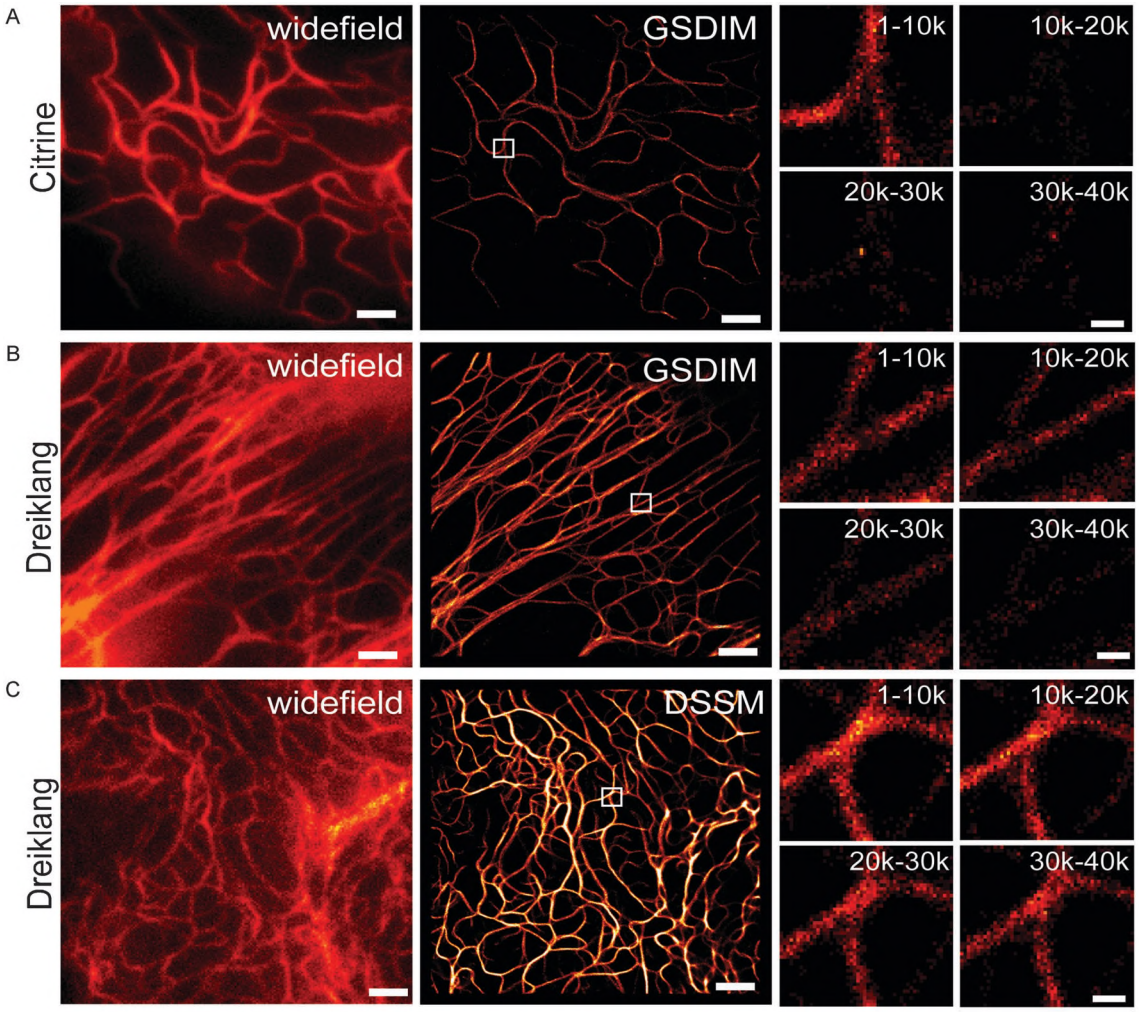

D

	Mean photon count	Event number frames 1-40k	Event number frames 1-10k	Event number frames 10k-20k	Event number frames 20k-30k	Event number frames 30k-40k
Citrine GSDIM	435	268,992	217,702	23,271	14,931	13,083
Dreiklang GSDIM	408	1,098,381	444,639	274,344	239640	139,842
Dreiklang DSSM	401	2,040,517	663,506	517,880	458,179	401,151

Figure 2. GSDIM and DSSM of HeLa cells expressing Vimentin–Citrine or Vimentin–Dreiklang: A) GSDIM of cells expressing Vimentin–Citrine. Large images, right: GSDIM image calculated from the first 40000 image frames; left: corresponding conventional widefield image. Small images: magnified GSDIM images from the area indicated in the large GSDIM image; each calculated from 10000 image frames, as indicated. B) GSDIM imaging of cells expressing Vimentin–Dreiklang. C) DSSM imaging of cells expressing Vimentin–Dreiklang. D) Table summarizing the mean number of detected photons per individual burst and the number of localization events in (A–C). Scale bars: 2 μm (large images), 200 nm (small images).

equipped with an oil immersion objective (HCX PL Apo 100x, NA 1.47) in the epifluorescence mode. For detection, an emission filter from 505–605 nm was used and images were collected with an Andor iXon camera (Andor Technology, Belfast, UK) over an area of $18 \times 18\ \mu m^2$. Up to 40000 frames with a frame rate of 100 Hz were recorded. The data sets were analyzed with the GSDIM analysis module of the Leica LASAF software. A detection threshold of 15 photons was used for event recognition. The final images were calculated using a pixel size of 20 nm in the histogram mode. For GSDIM imaging, the Dreiklang molecules were initially pumped into a dark state using 3 $kW\,cm^{-2}$ 488 nm light until single events were detectable (~10 s); subsequently, single molecules were imaged using the same light intensity. For DSSM, the sample was irradiated with blue light (100 $W\,cm^{-2}$, 405 nm) for one second to switch the proteins off, followed by imaging of single molecules with 488 nm light at 3 $kW\,cm^{-2}$. To increase the number of blinking events by switching Dreiklang on, the sample could be illuminated with 10 $W\,cm^{-2}$ UV light of 365–375 nm from a 100W Hg lamp.

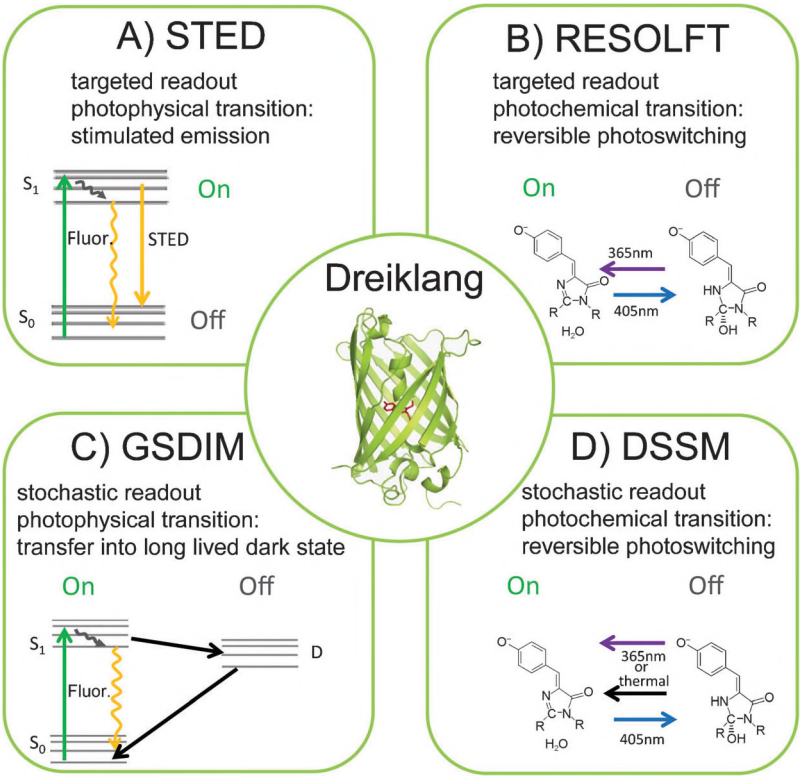

Figure 3. Nanoscopy with Dreiklang: The different approaches used and a schematic representation of the exploited light-driven switching mechanisms. A) STED: stimulated emission depletion microscopy. B) RESOLFT: reversible switchable optical linear (fluorescence) transitions microscopy. C) GSDIM: ground-state depletion followed by individual molecule return microscopy. D) DSSM: dreiklang stochastic switching microscopy. (A) and (B) rely on a targeted switching and read-out mode, whereas (C) and (D) use a stochastic switching and read-out approach.

STED Nanoscopy

STED nanoscopy was performed with a home-built setup, as described previously.[15] In brief, the excitation pulses of 488 nm and 100 ps duration were delivered by a pulsed-laser diode (Toptica Photonics, Graefelfing, Germany). The 300 ps STED pulses at 595 nm originated from an optical parametric oscillator (OPO, APE, Berlin, Germany) pumped by a Ti:Sapphire laser. A helical phase ramp was imprinted on the STED light by a polymeric phase plate (RPC Photonics, Rochester, NY) to produce a doughnut-shaped intensity profile in the focal plane. An NA 1.3 glycerol immersion objective was used (PL APO, CORR CS, 63x, glycerol, Leica Microsystems, Wetzlar, Germany) for the imaging. For the detection, an avalanche photodiode (PerkinElmer,Waltham, MA, USA) and a 535/50 nm band pass filter were used. An average power of 56 mW for the STED beam and 3.5 μW for the excitation beam measured at the back aperture of the objective were applied. Images were recorded with resonant mirror scanning (15 kHz, SC-30, Electro-Optical Products Corp., Ridgewood, NY, USA) along the *x* axis and stage scanning along the *y* axis (P-733, Physik Instrumente, Karlsruhe, Germany) with a pixel size of 20 nm and a dwell time of 10 μs.

RESOLFT Nanoscopy

RESOLFT nanoscopy was performed with a home-built confocal microscope setup similar to the one previously described.[10a] An NA 1.3 oil immersion objective lens (ACS APO 63x/1.3 OIL CS, Leica Microsystems, Wetzlar, Germany) was used for imaging. The diffraction-limited foci of the excitation beam and the beam for switching Dreiklang on were delivered by a 491 nm laser (Duo Calypso, Cobolt, Solna, Sweden, with a 491/10 nm bandpass and 532 nm notch filters) and a 355 nm laser (Zouk, Cobolt, Solna, Sweden, with a 355/10 nm filter), respectively. A 405 nm laser beam (DL100 diode laser, Toptica, Berlin, Germany) containing a 405/10 nm filter with circular polarization, after passing through a VPP-1b vortex plate (RPC Photonics, Rochester, NY) to imprint a 2π helical phase ramp, provided a doughnut-shaped focus with a central intensity minimum to switch Dreiklang off only at the focal rim. The irradiation times and intensities were controlled by acousto-optic modulators. An average power of 100 nW for the 355 nm beam (1 ms), 8 μW for the 405 nm beam (17 ms), and 350 nW for the 491 nm excitation beam (2 ms), measured at the back aperture of the objective, were applied. A piezo stage scanner was used for scanning the probe along the *xy* axes. Fluorescence was detected using a bandpass filter (550/88 nm) and an avalanche photodiode (SPCM-AQR-13, PerkinElmer, Waltham, MA).

Acknowledgements

We thank J. Jethwa for critical reading of the manuscript and T. Gilat and S. Löbermann for excellent technical assistance. We are indebted to the Bundesministerium für Bildung und Forschung (BMBF 513) for financial support in the program Optische Technologien für Biowissenschaften und Gesundheit (FKZ 13N11066; to SWH). Part of the work was supported by a Marie Curie Intra European Fellowship (to JGD) and by the Deutsche Forschungsgemeinschaft through the SFB 755 (to SJ) and the Cluster of Excellence "Nanoscale Microscopy and Molecular Physiology of the Brain" (to SWH and SJ).

Keywords: dreiklang · fluorescent proteins · nanoscopy · photoswitching · resolution

[1] a) B. Huang, H. Babcock, X. Zhuang, *Cell* **2010**, *143*, 1047–1058; b) D. Toomre, J. Bewersdorf, *Annu. Rev. Cell. Dev. Biol.* **2010**, *26*, 285–314.
[2] S. W. Hell, *Nat. Methods* **2009**, *6*, 24–32.
[3] a) S. W. Hell, S. Jakobs, L. Kastrup, *Appl. Phys. A* **2003**, *77*, 859–860; b) S. W. Hell, *Nat. Biotechnol.* **2003**, *21*, 1347–1355.
[4] S. W. Hell, J. Wichmann, *Opt. Lett.* **1994**, *19*, 780–782.
[5] M. Rust, M. Bates, X. Zhuang, *Nat. Methods* **2006**, *3*, 793–795.
[6] E. Betzig, G. H. Patterson, R. Sougrat, O. W. Lindwasser, S. Olenych, J. S. Bonifacino, M. W. Davidson, J. Lippincott-Schwartz, H. F. Hess, *Science* **2006**, *313*, 1642–1645.
[7] S. T. Hess, T. P. Girirajan, M. D. Mason, *Biophys. J.* **2006**, *91*, 4258–4272.
[8] a) J. Fölling, M. Bossi, H. Bock, R. Medda, C. A. Wurm, B. Hein, S. Jakobs, C. Eggeling, S. W. Hell, *Nat. Methods* **2008**, *5*, 943–945; b) M. Heilemann, S. van de Linde, M. Schuttpelz, R. Kasper, B. Seefeldt, A. Mukherjee, P.

Tinnefeld, M. Sauer, *Angew. Chem*. **2008**, *120*, 6266 – 6271; *Angew. Chem. Int. Ed.* **2008**, *47*, 6172 – 6176.
[9] D. Bourgeois, V. Adam, *IUBMB Life* **2012**, *64*, 482 – 491.
[10] a) T. Brakemann, A. C. Stiel, G. Weber, M. Andresen, I. Testa, T. Grotjohann, M. Leutenegger, U. Plessmann, H. Urlaub, C. Eggeling, M. C. Wahl, S. W. Hell, S. Jakobs, *Nat. Biotechnol.* **2011**, *29*, 942 – 947; b) T. Grotjohann, I. Testa, M. Leutenegger, H. Bock, N. T. Urban, F. Lavoie-Cardinal, K. I. Willig, C. Eggeling, S. Jakobs, S. W. Hell, *Nature* **2011**, *478*, 204 – 208.
[11] a) R. Ando, H. Hama, M. Yamamoto-Hino, H. Mizuno, A. Miyawaki, *Proc. Natl. Acad. Sci. USA* **2002**, *99*, 12651 – 12656; b) A. C. Stiel, S. Trowitzsch, G. Weber, M. Andresen, C. Eggeling, S. W. Hell, S. Jakobs, M. C. Wahl, *Biochem. J.* **2007**, *402*, 35 – 42.
[12] a) M. Andresen, A. C. Stiel, S. Trowitzsch, G. Weber, C. Eggeling, M. C. Wahl, S. W. Hell, S. Jakobs, *Proc. Natl. Acad. Sci. USA* **2007**, *104*, 13005 – 13009; b) M. Andresen, M. C. Wahl, A. C. Stiel, F. Gräter, L. V. Schäfer, S. Trowitzsch, G. Weber, C. Eggeling, H. Grubmüller, S. W. Hell, S. Jakobs, *Proc. Natl. Acad. Sci. USA* **2005**, *102*, 13070 – 13074.
[13] R. E. Thompson, D. R. Larson, W. W. Webb, *Biophys. J.* **2002**, *82*, 2775 – 2783.
[14] O. Griesbeck, G. S. Baird, R. E. Campbell, D. A. Zacharias, R. Y. Tsien, *J. Biol. Chem.* **2001**, *276*, 29188 – 29194.
[15] B. Hein, K. Willig, S. W. Hell, *Proc. Natl. Acad. Sci. USA* **2008**, *105*, 14271 – 14276.
[16] A. M. Bogdanov, E. A. Bogdanova, D. M. Chudakov, T. V. Gorodnicheva, S. Lukyanov, K. A. Lukyanov, *Nat. Methods* **2009**, *6*, 859 – 860.
[17] T. Dertinger, R. Colyer, G. Iyer, S. Weiss, J. Enderlein, *Proc. Natl. Acad. Sci. USA* **2009**, *106*, 22287 – 22292.
[18] S. Cox, E. Rosten, J. Monypenny, T. Jovanovic-Talisman, D. T. Burnette, J. Lippincott-Schwartz, G. E. Jones, R. Heintzmann, *Nat. Methods* **2012**, *9*, 195 – 200.